Acta Crystallographica Section F
Structural Biology and Crystallization Communications
ISSN 1744-3091

M. L. Rodrigues, T. Oliveira, P. M. Matias, I. C. Martins, F. M. A. Valente, I. A. C. Pereira and M. Archer*

Instituto de Tecnologia Química e Biológica, Universidade Nova de Lisboa, ITQB-UNL, Av. República, Apt. 127, 2781-901 Oeiras, Portugal

Correspondence e-mail: archer@itqb.unl.pt

Received 17 March 2006
Accepted 5 May 2006

Crystallization and preliminary structure determination of the membrane-bound complex cytochrome *c* nitrite reductase from *Desulfovibrio vulgaris* Hildenborough

The cytochrome *c* nitrite reductase (*c*NiR) isolated from *Desulfovibrio vulgaris* Hildenborough is a membrane-bound complex formed of NrfA and NrfH subunits. The catalytic subunit NrfA is a soluble pentahaem cytochrome *c* that forms a physiological dimer of about 120 kDa. The electron-donor subunit NrfH is a membrane-anchored tetrahaem cytochrome *c* of about 18 kDa molecular weight and belongs to the NapC/NirT family of quinol dehydrogenases, for which no structures are known. Crystals of the native *c*NiR membrane complex, solubilized with dodecylmaltoside detergent (DDM), were obtained using PEG 4K as precipitant. Anomalous diffraction data were measured at the Swiss Light Source to 2.3 Å resolution. Crystals belong to the orthorhombic space group $P2_12_12_1$, with unit-cell parameters a = 79.5, b = 256.7, c = 578.2 Å. Molecular-replacement and MAD methods were combined to solve the structure. The data presented reveal that *D. vulgaris* *c*NiR contains one NrfH subunit per NrfA dimer.

1. Introduction

Cytochrome *c* nitrite reductases (*c*NiR) usually perform the last step in nitrate ammonification, a dissimilatory process used by several organisms to grow anaerobically with nitrate as the terminal electron acceptor (reviewed in Potter *et al.*, 2001; Simon, 2002). In this last step, nitrite is reduced directly to ammonia in a six-electron reaction catalyzed by the pentahaem cytochrome *c* NrfA, for which several structures have been determined (Bamford *et al.*, 2002; Cunha *et al.*, 2003; Einsle *et al.*, 1999, 2000). The *c*NiR from the sulfate-reducing δ-proteobacterium *Desulfovibrio vulgaris* Hildenborough is unusual in that it is the first such enzyme to be isolated from an organism that does not perform nitrate ammonification (Pereira *et al.*, 2000). In this organism, *c*NiR is involved in nitrite detoxification, enabling it to overcome inhibition by this compound, which is produced by other organisms in the same habitat, such as nitrate-reducing sulfide-oxidizing bacteria (Greene *et al.*, 2003; Haveman *et al.*, 2004).

In *D. vulgaris*, the *c*NiR is found only in the form of a large membrane-bound complex of two subunits, identified in the genome as NrfA and the tetrahaem cytochrome *c* NrfH (Pereira *et al.*, 2000). The complex involves very strong interactions between NrfA and NrfH, since attempts to separate the two proteins were unsuccessful and led to degradation of the subunits. In *D. desulfuricans* ATCC 27774, which can grow by nitrate ammonification, the *c*NiR is also present only as a membrane-bound NrfHA complex that could be dissociated into the corresponding subunits in the presence of SDS (Almeida *et al.*, 2003; Pereira *et al.*, 1996). In the ε-proteobacteria *Wolinella succinogenes* and *Sulfurospirillum deleyianum*, NrfA is also associated with an NrfH protein, but the interaction between the two must be weaker since NrfA can be purified both as a membrane complex with NrfH or as an isolated protein in the periplasm or in the membrane fraction (Schumacher *et al.*, 1994; Simon *et al.*, 2000). In *Escherichia coli*, NrfA is always present as an isolated soluble protein and it receives electrons from another soluble pentahaem cytochrome NrfB (Clarke *et al.*, 2004).

The electrons used in nitrite reduction by the *c*NiR originate from the membrane quinone pool (Simon *et al.*, 2000; Tyson *et al.*, 1997). In the NrfHA *c*NiRs, the NrfH cytochrome is involved in direct electron transport between the quinone pool and NrfA (Simon *et al.*, 2000,

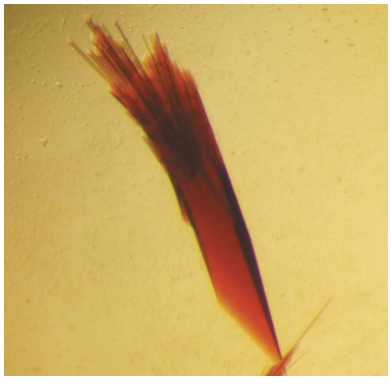

2001). NrfH is a membrane-bound cytochrome that contains a transmembrane helix at the N-terminus and a hydrophilic domain that binds four haems *c*. It belongs to a widespread family of membrane cytochromes, called the NapC/NirT family, that play an important function in anaerobic electron-transport chains, acting as quinol dehydrogenases and transferring electrons to a wide range of bacterial periplasmic reductases (Roldan *et al.*, 1998; Simon *et al.*, 2002). This family of cytochromes is more widely distributed among the proteobacteria than the bc_1 complex. The two best characterized members, NrfH and NapC, apparently have some differences in terms of the haem *c* axial ligands (Cartron *et al.*, 2002; Gross *et al.*, 2005) and only NrfH interacts directly with the terminal reductase (NrfA), with which it can form a strong complex. NrfH also seems to be more widely distributed among bacteria than NapC. Despite the importance of this family of cytochromes in respiratory electron-transfer chains, relatively few studies have been carried out with isolated proteins and no structural information is available. Here, we report the crystallization and preliminary structure determination of the NrfHA complex from *D. vulgaris* Hildenborough. This work will reveal the first structure of an NrfH cytochrome and will provide important insights into its interaction and mode of electron transfer with the quinone pool and NrfA.

2. Materials and methods

2.1. Protein production and purification

The *D. vulgaris* Hildenborough *c*NiR complex was purified from cell membranes using two protocols involving different detergents. The first made use of the zwitterionic sulfobetaine detergent SB12 [Zwittergent 3-12; 3-(*N*,*N*-dimethyldodecylammonio)-propanesulfonate] as previously described (Pereira *et al.*, 2000), but a final purification step on a Superdex S-200 was added. In the second protocol, membranes were extracted with the non-ionic detergent *n*-dodecyl-β-D-maltoside (DDM) according to Pires *et al.* (2006). The detergent extract was applied onto a Q-Sepharose Fast Flow column (5 × 30 cm; GE Healthcare) equilibrated with buffer containing 50 m*M* Tris–HCl pH 7.6, 10%(*v*/*v*) glycerol, 0.1%(*w*/*v*) DDM. A stepwise gradient of increasing NaCl concentration was performed and the fraction eluted at 50–100 m*M* NaCl was collected, concentrated and applied onto a Q-Sepharose HP column using the same buffers. The fraction eluted before the start of the gradient contained *c*NiR, which was further purified in a final passage on an S-200 HR column and eluted with 10 m*M* Tris–HCl pH 7.6, 100 m*M* NaCl, 0.1%(*w*/*v*) DDM. The purity of the two purified protein samples was assessed by UV–visible spectrum and SDS–PAGE stained with Coomassie and haem staining (Goodhew *et al.*, 1986).

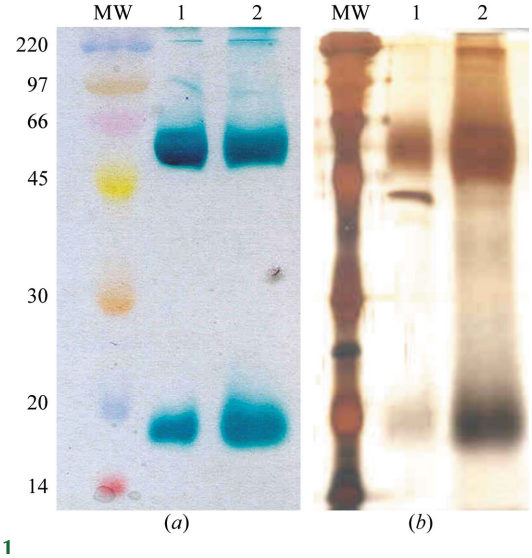

Figure 1
SDS–PAGE gels on protein solution and crystals. Gels were stained by haem staining (*a*) and with $AgNO_3$ (*b*). Gels were loaded with protein solution (lanes 1) and dissolved crystals (lanes 2). MW denotes the molecular-weight markers (molecular weights are shown in kDa). About ten needle-like crystals from the same drop were dissolved in the protein buffer solution and loaded onto each gel.

2.2. Crystallization

Protein samples were concentrated using an Amicon YM30 diaflow to about 10 mg ml^{-1} in 10 m*M* Tris–HCl pH 7.5 buffer containing either 0.03%(*w*/*v*) DDM or 0.2%(*w*/*v*) Zwittergent 3-12. Initial crystallization conditions were determined using a grid screen with 5–20%(*w*/*v*) PEG 4K as precipitant, buffers of varying pH and additives. These experiments, performed at 277 and 293 K, were based on previously described crystallization conditions for the NrfA subunit from other sources. Crystals were obtained from protein samples with both detergents, but the results with DDM were more promising. Crystals were grown at 277 K by the vapour-diffusion technique by mixing equal amounts (1.5 µl) of protein and reservoir solution, which contained about 10%(*w*/*v*) PEG 4K in 0.1 *M* HEPES pH 7.5 buffer. Crystals appeared within one to three weeks and grew in parallelepiped shapes to maximum dimensions of about 0.30 × 0.20 × 0.10 mm or in long needles ~0.05 mm thick. The presence of both subunits, the *c*-type cytochromes NrfA and NrfH, was confirmed by SDS–PAGE on the dissolved crystals (Fig. 1).

2.3. X-ray data collection and analysis

The *c*NiR crystal shown in Fig. 2 was treated by the gradual addition of cryoprotectant solution (14% PEG 4K, 0.1 *M* HEPES pH 7.5, 30 m*M* glycyl-glycyl-glycine, 20% glycerol) at 30 min intervals until the glycerol concentration reached about 20%. This crystal was then transferred to a new drop containing the cryoprotectant solution and flash-cooled in liquid nitrogen.

X-ray data were measured at the Swiss Light Source synchrotron on the tunable beamline PXI (X06AS), which is equipped with a MAR 225 mosaic CCD detector. A fluorescence scan around the Fe *K* edge was performed prior to a multiple-wavelength anomalous

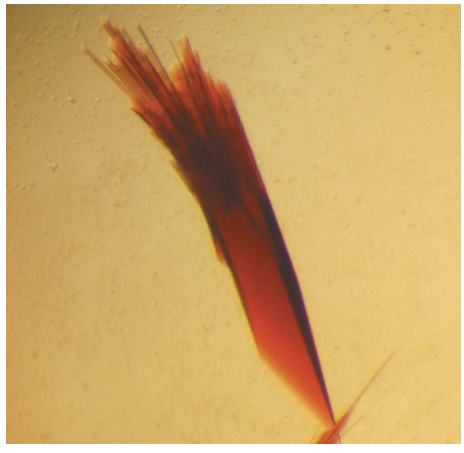

Figure 2
A crystal of the *c*NiR complex. The native crystal was grown at 277 K using PEG 4K as precipitant and glycyl-glycyl-glycine as additive. The crystal grew to dimensions of ~0.60 × 0.20 × 0.10 mm in approximately three weeks.

Table 1
Statistics of data processing and phasing.

The space group was $P2_12_12_1$, with unit-cell parameters a = 79.4, b = 256.8, c = 579.2 Å.
(*a*) Data processing.

	Peak	Inflection	Remote
Wavelength (Å)	1.7393	1.7408	0.9000
Resolution range (Å)	64.0–2.60 (2.74–2.60)	55.3–2.60 (2.74–2.60)	54.0–2.30 (2.42–2.30)
Completeness, overall (%)	85.2 (45.2)	85.1 (44.4)	83.9 (67.3)
Completeness, anomalous (%)	62.4 (15.4)	65.7 (17.7)	67.3 (33.4)
No. of observations	972147 (36782)	1023754 (38166)	1279751 (107004)
No. of unique reflections	310637 (23876)	311156 (23563)	443656 (51436)
Redundancy, overall	3.1 (1.5)	3.3 (1.6)	2.9 (2.1)
Redundancy, anomalous	1.9 (1.3)	1.9 (1.3)	1.7 (1.5)
$R_{\rm sym}$† (%)	6.8 (14.7)	7.6 (19.2)	9.8 (31.0)
$R_{\rm anom}$ (%)	6.1 (12.7)	5.8 (13.5)	8.0 (22.1)
$\langle I/\sigma(I)\rangle$	13.7 (4.6)	12.8 (4.0)	8.3 (3.1)

(*b*) *SHARP* phase determination and refinement.

	Peak		Inflection		Remote	
	Acentric	Centric	Acentric	Centric	Acentric	Centric
Phasing power, isomorphous	1.78	1.40	2.20	1.79	0.00	0.00
Phasing power, anomalous	0.78	—	0.62	—	0.14	—
$R_{\rm cullis}$, isomorphous	0.476	0.515	0.400	0.431	0.00	0.00
$R_{\rm cullis}$, anomalous	0.867	—	0.908	—	0.994	—
Mean figure of merit, acentric	0.465					
Mean figure of merit, centric	0.450					

† $R_{\rm sym} = \sum_h \sum_i [|I_i(h) - \langle I(h)\rangle|/\sum_h \sum_i I_i(h)]$, where I_i is the ith measurement and $\langle I(h)\rangle$ is the weighted mean of all measurements of $I(h)$.

dispersion (MAD) experiment. X-ray diffraction data were collected just above the iron absorption peak ($\lambda_{\rm pk}$ = 1.7393 Å), at the inflection point of the fluorescence curve ($\lambda_{\rm ip}$ = 1.7408 Å) and at a high-energy remote wavelength ($\lambda_{\rm rem}$ = 0.9000 Å), with an oscillation angle of 0.25° and an exposure time of 1 s per frame. The crystal was translated a few times during data collection to minimize the effects of radiation damage. The crystal diffracted to beyond 2.3 Å resolution and belonged to the orthorhombic space group $P2_12_12_1$, with unit-cell parameters a = 79.5, b = 256.7, c = 578.2 Å. Data were processed with *MOSFLM* (Leslie, 1992) and merged with *SCALA* from the *CCP*4 program suite (Collaborative Computational Project, Number 4, 1994). Data-collection and processing statistics are listed in Table 1.

Depending on the number of complex molecules (5–8) present in the asymmetric unit and the stoichiometry of the complex (either 2:2 or 2:1 NrfA:NrfH), the Matthews coefficient (Matthews, 1968) and the solvent content may range from 2.3 to 4.2 Å^3 Da^{-1} and from 46.3 to 70.6%, respectively.

2.4. Preliminary structure determination

The three-dimensional structure of the *D. vulgaris c*NiR complex was solved by a combination of molecular replacement and MAD phasing. The structure of the larger subunit NrfA (~60 kDa) was solved with *Phaser* (McCoy *et al.*, 2005) using the coordinates of the NrfA dimer from *D. desulfuricans* (PDB code 1oah, with an amino-acid sequence identity of 66%) as the search model. Six such NrfA dimers were found in the asymmetric unit of the crystal structure of the *D. vulgaris* NrfHA complex. An anomalous Fourier map was then calculated using the phases from the molecular-replacement solution of the NrfA dimer substructure and the anomalous difference coefficients obtained from the peak data set. 24 Fe atoms from the unknown smaller (~18 kDa) NrfH subunit were located from this map.

The 84 iron sites present in the asymmetric unit, corresponding to 12 molecules of NrfA and six molecules of NrfH, were then input into *SHARP* (de La Fortelle & Bricogne, 1997) for a maximum-likelihood heavy-atom parameter refinement based on the three-wavelength MAD data set. To minimize bias, the phases from the molecular-replacement calculations were not used. The final statistics from the *SHARP* calculations are included in Table 1. The resulting phases were further improved using a density-modification procedure including solvent-content optimization with *SOLOMON* (Abrahams & Leslie, 1996) and *DM* (Cowtan, 1994). These calculations led to an optimized solvent content of 58.8% and a final correlation coefficient on $|E^2|$ of 0.792.

3. Results and discussion

The crystallization of the *D. vulgaris* cytochrome *c* nitrite reductase complex (NrfHA) involved great experimental effort owing to the non-reproducibility of crystal growth and the unreliability of diffraction quality for crystals that were grown under similar conditions. Although crystals appeared in several drops containing PEG 4K at pH values around 7.5, most crystals diffracted poorly. Crystal optimization involved variation of the type of precipitant, the precipitant and protein concentrations and ratios, the pH, additives and temperature. Different crystallization methods (vapour diffusion, microbatch, agarose gels) and seeding techniques were also attempted. Many crystallization trials and crystals had to be screened before a good diffraction-quality crystal was found. The crystal in Fig. 2 was obtained from a sitting-drop vapour-diffusion experiment containing 5 mg ml^{-1} protein, 0.015% DDM detergent, 10% PEG 4K, 0.1 *M* HEPES pH 7.5 and 30 m*M* glycyl-glycyl-glycine as an additive. It is worth mentioning that of the ~100 crystals tested so far, we have only found three or four crystals that diffract to a resolution of ~3 Å at a synchrotron source (ESRF, DESY, SLS). The growth of good diffracting crystals appears to be fortuitous; the conditions that favour the formation of well ordered crystals are still not completely understood.

NrfHA crystals were also sensitive to the addition of the cryoprotectant solution. Several compounds were tested for efficient cryocooling, including 2,3-butanediol, glycerol, PEG 400, ethylene glycol, MPD and oils (paraffin oil and Paratone-N from Hampton Research and Panjelly from Jena Bioscience). The slow addition of glycerol cryoprotectant showed to be a suitable protocol for NrfHA crystals, as high-quality diffraction data were obtained from a crystal diffracting to beyond 2.3 Å at a synchrotron source.

The presence of a very long unit-cell axis (∼580 Å) was a significant obstacle to optimal data collection. This long unit-cell axis lies perpendicular to the longest crystal axis and owing to technical constraints it was not possible to orient the crystal with the longest axis close to the spindle axis (Fig. 3). Also, limitation of data-collection time did not allow the use of smaller oscillation angles. As a result, some spot-overlap problems were expected during data processing, although crystal mosaicity was low (0.2–0.3°). Of the several data-processing packages used to attempt to integrate, scale and merge the diffraction data, the best results were clearly achieved with *MOSFLM*, since its dynamic profile algorithm could best resolve the spatial overlap problems caused by the large unit-cell parameters and the unfavourable crystal orientation. In this way, it was possible to obtain peak and inflection-point data sets to 2.6 Å and a remote data set to 2.3 Å.

The preliminary structure of the NrfHA complex, determined by a combination of molecular replacement for NrfA and MAD for NrfH, reveals a 2:1 stoichiometry between the two cytochrome *c* proteins, as previously proposed for *D. desulfuricans* *c*NiR (Almeida *et al.*, 2003). In contrast, a 2:2 NrfA:NrfH arrangement has been assumed to be the most likely form of *W. succinogenes* *c*NiR (Einsle, Messerschmidt *et al.*, 2002; Einsle, Stach *et al.*, 2002).

The 2.3 Å electron-density maps resulting from phase determination and refinement using *SHARP* followed by a density-modification procedure including solvent-content optimization were of good quality and allowed the building of the six NrfH molecules and the rebuilding of the 12 NrfA molecules in the crystal asymmetric unit. Further crystallographic refinement is under way.

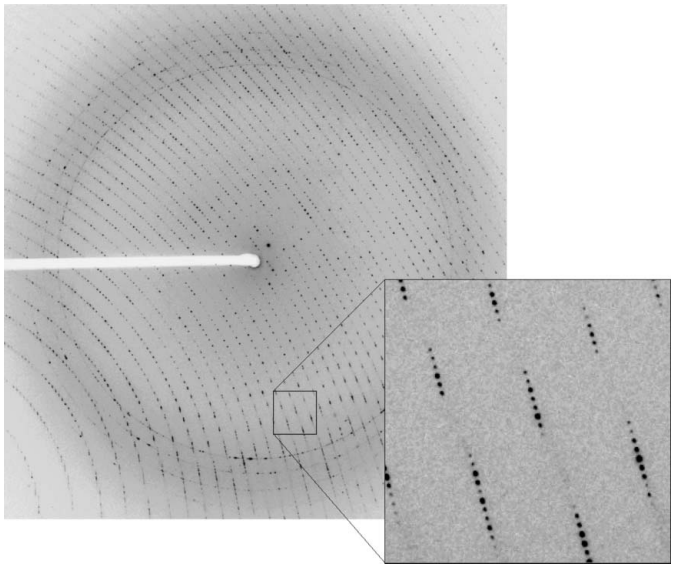

Figure 3
X-ray diffraction image recorded at the SLS synchrotron. Diffraction pattern at 2.3 Å resolution at the detector corner (high-energy remote wavelength). An enlargement of the diffraction pattern at ∼4.5–5 Å resolution shows very close reflection spots along the longest unit-cell axis.

The authors would like to thank Clemens Schulze-Briese for assistance with data collection at the Swiss Light Source, PSI, Villigen. Travel to SLS was supported by the European Commission under the Sixth Framework Programme through the Key Action Strengthening the European Research Area, Research Infrastructures, contract No. RII3-CT-2004-506008. MLR is the recipient of an FCT-POCTI fellowship (SFRH/BPD/24372/2005). This work was supported by FCT grant POCTI/2002/ESP/44782.

References

Abrahams, J. P. & Leslie, A. G. W. (1996). *Acta Cryst.* D**52**, 30–42.
Almeida, M. G., Macieira, S., Goncalves, L. L., Huber, R., Cunha, C. A., Romao, M. J., Costa, C., Lampreia, J., Moura, J. J. & Moura, I. (2003). *Eur. J. Biochem.* **270**, 3904–3915.
Bamford, V. A., Angove, H. C., Seward, H. E., Thomson, A. J., Cole, J. A., Butt, J. N., Hemmings, A. M. & Richardson, D. J. (2002). *Biochemistry*, **41**, 2921–2931.
Cartron, M. L., Roldan, M. D., Ferguson, S. J., Berks, B. C. & Richardson, D. J. (2002). *Biochem. J.* **368**, 425–432.
Clarke, T. A., Dennison, V., Seward, H. E., Burlat, B., Cole, J. A., Hemmings, A. M. & Richardson, D. J. (2004). *J. Biol. Chem.* **279**, 41333–41339.
Collaborative Computational Project, Number 4 (1994). *Acta Cryst.* D**50**, 760–763.
Cowtan, K. (1994). *Jnt CCP4/ESF–EACBM Newsl. Protein Crystallogr.* **31**, 34–38.
Cunha, C. A., Macieira, S., Dias, J. M., Almeida, G., Goncalves, L. L., Costa, C., Lampreia, J., Huber, R., Moura, J. J., Moura, I. & Romao, M. J. (2003). *J. Biol. Chem.* **278**, 17455–17465.
Einsle, O., Messerschmidt, A., Huber, R., Kroneck, P. M. & Neese, F. (2002). *J. Am. Chem. Soc.* **124**, 11737–11745.
Einsle, O., Messerschmidt, A., Stach, P., Bourenkov, G. P., Bartunik, H. D., Huber, R. & Kroneck, P. M. (1999). *Nature (London)*, **400**, 476–480.
Einsle, O., Stach, P., Messerschmidt, A., Klimmek, O., Simon, J., Kroger, A. & Kroneck, P. M. (2002). *Acta Cryst.* D**58**, 341–342.
Einsle, O., Stach, P., Messerschmidt, A., Simon, J., Kroger, A., Huber, R. & Kroneck, P. M. (2000). *J. Biol. Chem.* **275**, 39608–39616.
Goodhew, C. F., Brown, K. R. & Pettigrew, G. W. (1986). *Biochim. Biophys. Acta*, **852**, 288–294.
Greene, E. A., Hubert, C., Nemati, M., Jenneman, G. E. & Voordouw, G. (2003). *Environ. Microbiol.* **5**, 607–617.
Gross, R., Eichler, R. & Simon, J. (2005). *Biochem. J.* **390**, 689–693.
Haveman, S. A., Greene, E. A., Stilwell, C. P., Voordouw, J. K. & Voordouw, G. (2004). *J. Bacteriol.* **186**, 7944–7950.
La Fortelle, E. de & Bricogne, G. (1997). *Methods Enzymol.* **276**, 472–494.
Leslie, A. G. W. (1992). *Jnt CCP4/ESF–EACBM Newsl. Protein Crystallogr.* **26**.
McCoy, A. J., Grosse-Kunstleve, R. W., Storoni, L. C. & Read, R. J. (2005). *Acta Cryst.* D**61**, 458–464.
Matthews, B. W. (1968). *J. Mol. Biol.* **33**, 491–497.
Pereira, I. C., Abreu, I. A., Xavier, A. V., LeGall, J. & Teixeira, M. (1996). *Biochem. Biophys. Res. Commun.* **224**, 611–618.
Pereira, I. A., LeGall, J., Xavier, A. V. & Teixeira, M. (2000). *Biochim. Biophys. Acta*, **1481**, 119–130.
Pires, R. H., Venceslau, S. S., Morais, F., Teixeira, M., Xavier, A. V. & Pereira, I. A. C. (2006). *Biochemistry*, **45**, 249–262.
Potter, L., Angove, H., Richardson, D. & Cole, J. (2001). *Adv. Microb. Physiol.* **45**, 51–112.
Roldan, M. D., Sears, H. J., Cheesman, M. R., Ferguson, S. J., Thomson, A. J., Berks, B. C. & Richardson, D. J. (1998). *J. Biol. Chem.* **273**, 28785–28790.
Schumacher, W., Hole, U. & Kroneck, M. H. (1994). *Biochem. Biophys. Res. Commun.* **205**, 911–916.
Simon, J. (2002). *FEMS Microbiol. Rev.* **26**, 285–309.
Simon, J., Eichler, R., Pisa, R., Biel, S. & Gross, R. (2002). *FEBS Lett.* **522**, 83–87.
Simon, J., Gross, R., Einsle, O., Kroneck, P. M., Kroger, A. & Klimmek, O. (2000). *Mol. Microbiol.* **35**, 686–696.
Simon, J., Pisa, R., Stein, T., Eichler, R., Klimmek, O. & Gross, R. (2001). *Eur. J. Biochem.* **268**, 5776–5782.
Tyson, K., Metheringham, R., Griffiths, L. & Cole, J. (1997). *Arch. Microbiol.* **168**, 403–411.